On the uncertainty of the Auger recombination coefficient extracted from InGaN/GaN light-emitting diode efficiency droop measurements

Joachim Piprek,[1,a)] Friedhard Römer,[2] and Bernd Witzigmann[2]
[1]*NUSOD Institute LLC, Newark, Delaware 19714-7204, USA*
[2]*Department of Electrical Engineering, University of Kassel, 34121 Kassel, Germany*

(Received 23 December 2014; accepted 28 February 2015; published online 10 March 2015)

III-nitride light-emitting diodes (LEDs) suffer from a severe efficiency reduction with increasing injection current (droop). Auger recombination is often seen as primary cause of this droop phenomenon. The corresponding Auger recombination coefficient C is typically obtained from efficiency measurements using mathematical models. However, C coefficients reported for InGaN active layers vary over two orders of magnitude. We here investigate this uncertainty and apply successively more accurate models to the same efficiency measurement, thereby revealing the strong sensitivity of the Auger coefficient to quantum well properties such as electron-hole ratio, electric field, and hot carrier escape. © *2015 AIP Publishing LLC*.
[http://dx.doi.org/10.1063/1.4914833]

State-of-the-art GaN-based light-emitting diodes (LEDs) deliver the desired high efficiency only at relatively low light power. At the elevated injection current required in practical high-power applications, the internal quantum efficiency (IQE) is substantially reduced. This efficiency droop phenomenon originates in carrier loss mechanisms, which prevent electron-hole pairs from generating photons inside the active layers.[1] Among the proposed droop mechanisms are Auger recombination,[2] electron leakage,[3] and density-activated defect recombination (DADR).[4] We here focus exclusively on Auger recombination. First direct experimental evidence for Auger recombination in blue LEDs was recently provided,[5,6] but the magnitude of this recombination process remains unclear. Quantitative evaluations of the Auger mechanism are mainly based on the modeling of measured efficiency characteristics and lead to a large variation of extracted Auger coefficients C (Fig. 1). This variation is hardly investigated in the literature, but it creates a major uncertainty in the analysis of the efficiency droop. In this paper, we discuss several reasons for C-parameter discrepancies and successively apply more accurate models to the same efficiency measurement. We thereby reveal that the extracted Auger coefficient is very sensitive to the assessment of quantum well properties such as the carrier density, the electron-hole ratio, the overlap of confined wave functions, the polarization field, and the escape of hot carriers.

The most popular model is the so-called ABC model which describes the measured external quantum efficiency EQE by the formula

$$\mathrm{EQE} = \mathrm{EXE} \times \mathrm{IQE} = \mathrm{EXE} \times \mathrm{INE} \times \mathrm{Bn}^2/(\mathrm{An} + \mathrm{Bn}^2 + \mathrm{Cn}^3), \quad (1)$$

with the photon extraction efficiency EXE, the quantum well (QW) injection efficiency INE, and the carrier recombination rate inside the QWs given by a third order power series $\mathrm{R(n)} = \mathrm{An} + \mathrm{Bn}^2 + \mathrm{Cn}^3$ as function of the carrier density n. The coefficients A, B, and C are associated with defect-related Shockley-Read-Hall (SRH) recombination, spontaneous photon emission, and Auger recombination, respectively. The efficiency is usually plotted over the current density $\mathrm{j} = \mathrm{qdR(n)}$ with the electron charge q and the total thickness of active layers d. The injection efficiency accounts for recombination outside the active layers (carrier leakage), which is often neglected (INE = 1). With such ABC model, the third-order parameter C is the only one that is responsible for the efficiency droop at high current densities since the recombination rate Cn^3 is the only one that is rising faster than the photon emission rate Bn^2 with increasing carrier density.

Based on this and similar models, a large variety of C-parameters was extracted from efficiency measurements. Figure 1 shows published data for single active layers[2,7–9] and for multiple quantum wells (MQWs).[10–15] The carrier density n is typically determined using carrier lifetime measurements. MQW active regions cause a major uncertainty with the simple ABC model (1), because their QWs are

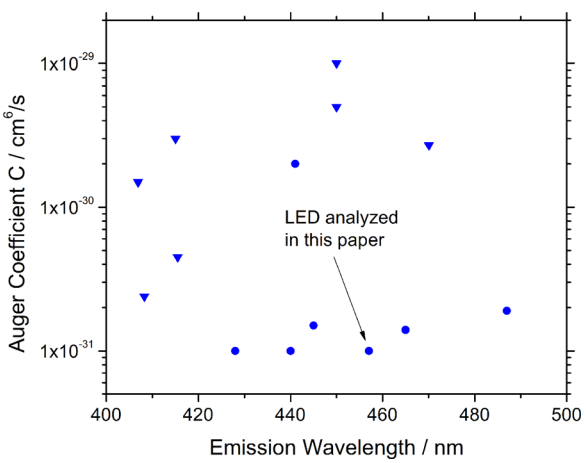

FIG. 1. Published Auger coefficients C extracted from measurements on devices with InGaN active layers of different emission wavelength (circles—single active layer, triangles—multiple quantum wells).

[a)]piprek@nusod.org

known to exhibit different carrier densities.[16] We therefore focus our attention on single quantum well (SQW) LEDs, in particular, on electro-luminescence and differential carrier lifetime measurements performed on an industry-grade 3 nm SQW LED emitting light at 457 nm wavelength.[8] This device exhibits its peak quantum efficiency at a current density of $j_{peak} = 5\ A/cm^2$ (Fig. 2). The IQE maximum of about 75% was determined from the measured EQE peak by assuming INE = 1 and independently calculating the photon extraction efficiency EXE.[8] The differential carrier lifetime τ_{diff} is given by $1/\tau_{diff} = dR/dn = A + 2Bn + 3Cn^2$. Our fit of the ABC model to these measurements results in the solid lines in Fig. 2 using the recombination parameters listed in the top row of Table I. B and C are in good agreement with our reference; the A parameter was not reported.[8]

However, as previously discussed,[17] various ABC parameter sets give identical IQE characteristics and large variations of the extracted Auger parameter are possible if the QW carrier density is not exactly known (Fig. 3). In our case, the lifetime τ_{diff} was measured at different current densities from the emission decay after a small current pulse.[8] Within the framework of the simple ABC model, this method provides rather accurate values for the SQW carrier density and for the corresponding recombination coefficients (vertical line in Fig. 3). Other methods are accompanied by a larger error.[2] Some reported ABC analyses ignore this issue and simply assume a specific value for one of the ABC parameters.

Many variations of the ABC model have been proposed in the literature.[18] Some groups consider carrier leakage as possible cause of the droop by adding higher-order terms or f(n) to R(n).[19] Other authors introduce declining coefficients B(n) and C(n) to account for high-density effects that are also observed in microscopic recombination models.[20,21] All these ABC model modifications introduce additional unknown parameters and lead to different sets of extracted recombination coefficients.

For a more detailed evaluation of the recombination processes, let us now apply a more general recombination formula, which distinguishes between the densities n and p for electron and holes, respectively,[22]

TABLE I. Recombination parameter sets extracted from the measurements in Fig. 2 using different models.

Model	$A/10^6\ s^{-1}$	$B/10^{-12}\ cm^3/s$	$C/10^{-31}\ cm^6/s$
ABC model	2.6	3.0	1.0
ABC model with n = 2p	3.9	1.5	0.16
APSYS	14[a]	(17[a])	2.5[a]
Quatra/Cels	3.1	4.1[b]	1.7[b]
Quatra/Cels (hot carriers)	3.1	4.1[b]	0.8[b]
Quatra/Cels (no polarization)	5.9	17.7	7.0

[a]Electron-hole separation is considered separately.
[b]Values B(j) and C(j) given at $j_{peak} = 5\ A/cm^2$.

$$R(n,p) = (np - n_0p_0)/(\tau_p(n+n_1) + \tau_n(p+p_1)) + B\,(np - n_0p_0) + (C_n n + C_p p)(np - n_0p_0), \quad (2)$$

with the SRH lifetimes $\tau_{n,p}$ for electrons and holes, respectively. The Auger coefficients $C_{n,p}$ account for the two possible Auger processes, transferring the recombination energy to an electron in the conduction bands and a hole in the valence bands, respectively. The equilibrium carrier density product n_0p_0 is much smaller than np in a QW under operating conditions. The defect parameters n_1 and p_1 are also often neglected. For simplicity, we here set $\tau_n = \tau_p = \tau_{SRH}$, $A = 1/2\tau_{SRH}$, and $C = C_n = C_p$. With n = p, we then arrive at the ABC recombination model used in (1).

However, differences in electron and hole confinement inside the quantum well are to be expected,[23,24] especially with strong built-in polarization fields and poor hole injection, both typical for GaN-based LEDs. For a simple comparison, let us assume n = 2p. The ABC formula for the internal quantum efficiency then changes to $IQE = INE \times 2Bp^2 / (2Ap/3 + 2Bp^2 + 6Cp^3)$. Obviously, without further computation, the previously determined recombination parameters can be changed by fixed factors to obtain the new ABC fit parameters given in Table I, including a significantly smaller Auger coefficient.

For a more thorough analysis, we now employ different numerical device simulation packages to analyze the IQE

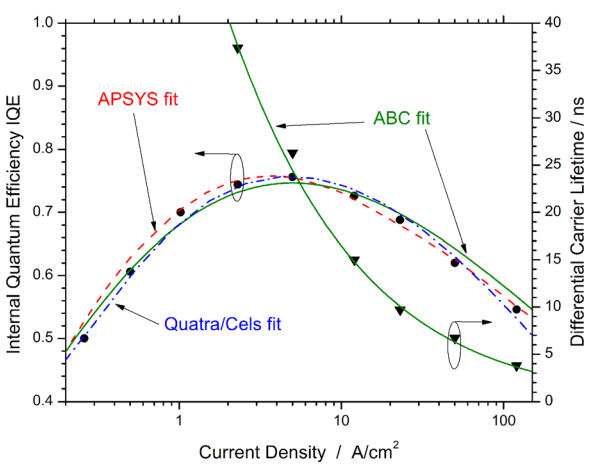

FIG. 2. Internal quantum efficiency IQE and differential carrier lifetime as function of current density (symbols—measurements, lines—modeling).

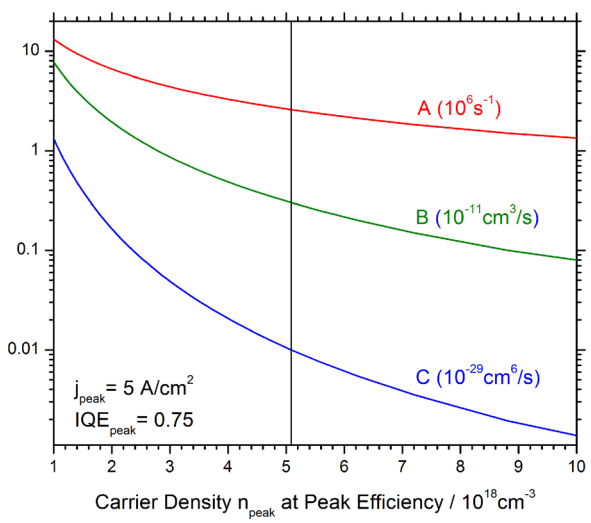

FIG. 3. ABC parameter sensitivity to the quantum well carrier density at the IQE peak. Each vertical parameter combination gives identical IQE curves in Fig. 2. The vertical line corresponds to the lifetime fit in Fig. 2.

measurement in Fig. 2. The first package is the APSYS software,[25] which self-consistently combines carrier transport and QW recombination.[26] The model accounts for the QW potential deformation by the built-in polarization field and the corresponding separation of electrons and holes (Fig. 4). The polarization is computed using a second-order model that gives a SQW interface polarization charge density of $1.8 \times 10^{13}\,cm^{-2}$ and a built-in SQW polarization field of about 3 MV/cm in our case.[27] After considering the screening by free and confined carriers, the simulated average QW field strength is still about 2.6 MV/cm at the efficiency peak and about 1.9 MV/cm at 150 A/cm^2. At the IQE peak, the average QW carrier density is $14 \times 10^{18}\,cm^{-3}$ for electrons and $6 \times 10^{18}\,cm^{-3}$ for holes, giving an electron-hole ratio of 2.3, close to our previous assumption.

APSYS computes the QW spontaneous emission spectrum self-consistently from the wave functions and the QW band structure, which is represented by a 6×6 k•p model. Using a QW Indium content of 16%, the measured emission peak of 457 nm is reproduced in the simulation. The total emission rate is obtained at every bias point by integrating the emission spectrum, thereby eliminating B as free fit parameter. The non-radiative recombination rates are calculated from the QW carrier distributions n(x) and p(x) as shown in Fig. 4 using the terms given in Eq. (2). Fitting of the measured efficiency data results in $\tau_{SRH} = 36$ ns, $A = 14 \times 10^6\,s^{-1}$, and $C = 2.5 \times 10^{-31}\,cm^6/s$ (dashed line in Fig. 2). An almost identical fit is obtained by using the simple emission rate Bnp with $B = 17 \times 10^{-12} cm^3/s$. Since the electron-hole separation is considered separately in Eq. (2), these numbers are substantially larger than the ABC parameters extracted earlier (see Table I).

However, the employment of QW wave-function weighted 3-dimensional (3D) carrier densities n(x) and p(x) in (2) leads to recombination rate profiles inside the QW, which misrepresent the actual interaction of the entire confined carrier wave functions in QW recombination processes. Similar to the QW photon emission model, non-radiative recombination models should include the whole carrier wave functions and use 2D carrier densities [cm^{-2}] in connection with a 2D C-parameter [cm^4/s] as in

$$R_{Aug2D} = (C_{n2D} n_{2D} + C_{p2D} p_{2D})(n_{2D} p_{2D} - n_{02D} p_{02D}). \quad (3)$$

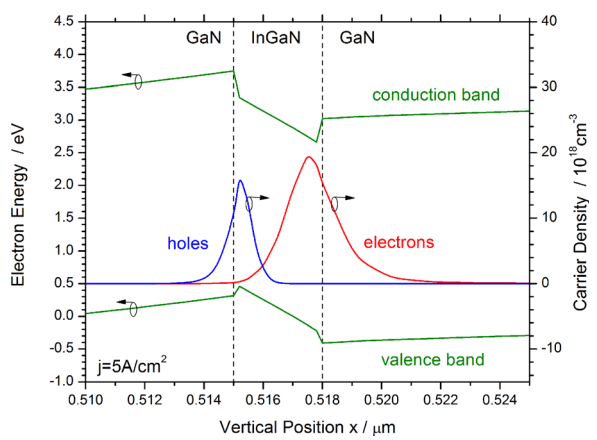

FIG. 4. Quantum well energy band diagram and carrier density profiles at $j_{peak} = 5$ A/cm^2 as calculated with APSYS.

This 2D Auger recombination rate can be translated into the common 3D rate using the QW thickness d and $R_{Aug} = R_{Aug2D}/d$. The resulting 3D Auger coefficient $C = d^2 C_{2D}$ includes the separation of electrons and holes inside the QW. As this separation is a function of the electric field, C changes with increasing bias, i.e., the Auger coefficient becomes a function of the current density.

Such improved 2D recombination model is implemented in the second numerical device simulation package employed in our study, Quatra/Cels,[28] which also solves the coupled system of Poisson, electron/hole continuity, and Schrödinger equation self-consistently. The 2D-carrier population in the QW follows a separate carrier continuity equation, which couples to the barrier levels via an in- and out-scattering term.[29] The bound carrier densities enter the Poisson equation following the QW envelope wave functions in quantized direction. The Auger coefficient includes the overlap integrals of the envelope wave functions.[30] The same principle is applied to the spontaneous emission rate, although the calculation of this rate also includes a spectral integration within a free carrier perturbation theory with an energy band structure from a k•p model. The SRH recombination model does not consider the wave function overlap integral, as we believe that the defect distribution in the barrier-well system is not constant. Here, more advanced models including interface effects need to be developed. Using this approach, the IQE measurement in Fig. 2 can be fitted quite well (dashed-dotted line in Fig. 2). B and C now rise by 20% and 50%, respectively, in the current density range shown in Fig. 2, as the QW electric field and the electron-hole separation are reduced. Table I lists both parameters at the IQE peak.

The Quatra/Cels software also allows for the escape of hot carriers generated by the QW Auger recombination.[31] In that case, the QW recombination rate (3) underestimates the carrier loss due to Auger recombination. The hot carrier is added to the bulk distribution, or in a worst case scenario, to the minority contact current as leakage. In the latter case, the IQE fit results in half of the C parameter for the hot carrier leakage effect (see Table I). More detailed carrier transport investigations are needed to establish the actual hot carrier escape ratio in our case.

Numerical simulations of GaN-LEDs often include a scaling factor (<1) for the built-in polarization, which accounts for screening by charged interface defects.[32] Such factor reduces the built-in QW field, lowers the electron-hole separation, and leads to stronger recombination. Since the density of charged QW interface defects is unknown, we, here, only consider the extreme case without QW polarization in which the electron-hole separation inside the QW is eliminated and the B and C parameters do not change with current any more (see last row in Table I). The A and C parameters extracted from the efficiency measurement are now substantially higher, because they need to compensate for the stronger photon emission.

Microscopic theories of *direct* Auger recombination in III–V semiconductors traditionally predict negligibly low C-parameters for wide-gap materials, partially based on simplified band structure models.[33] Much higher C coefficients were recently computed for *indirect* Auger

transitions in *bulk* InGaN,[34] resulting in $C_n = 0.7 \times 10^{-31}\,cm^6/s$ and $C_p = 1.2 \times 10^{-31}\,cm^6/s$ in our case. However, modeling details are still debated and other authors predict smaller bulk C coefficients for our InGaN band gap.[35] Calculations for InGaN quantum wells are more complicated and preliminary results are published only for *direct* Auger recombination, none of which is comparable to our case. Based on advanced band structure models, some of those reports indicate a strong influence of the QW width[36] as well as enhanced Auger recombination with rising electric field.[37] Other models predict C-parameter reductions with graded QW interfaces.[38] Thus, existing microscopic models confirm the strong influence of QW properties on the Auger recombination and the inapplicability of bulk material parameters.

In conclusion, the popular ABC model (1) is not sufficient to obtain a consistent value for the Auger coefficient C from efficiency measurements. The extracted C-parameter strongly depends on quantum well properties such as electron-hole ratio, net polarization field, and hot carrier escape ratio. We demonstrate how the successive application of more detailed models provides a deeper understanding and a more accurate quantitative assessment of the Auger recombination process. However, more detailed models require more detailed information on quantum well properties, some of which are not available in our case. Based on the existing information,[8] we are also unable to evaluate the influence of other effects such as current crowding,[10] electron leakage,[3] non-uniform Indium distribution,[39] or excitonic enhancement.[40] Further research is needed to fully understand the contribution of Auger recombination to the GaN-LED efficiency droop.

[1] J. Piprek, Phys. Status Solidi A **207**, 2217–2225 (2010).
[2] Y. C. Shen, G. O. Mueller, S. Watanabe, N. F. Gardner, A. Munkholm, and M. R. Krames, Appl. Phys. Lett. **91**, 141101 (2007).
[3] M. H. Kim, M. F. Schubert, Q. Dai, J. K. Kim, E. F. Schubert, J. Piprek, and Y. Park, Appl. Phys. Lett. **91**, 183507 (2007).
[4] J. Hader, J. V. Moloney, and S. W. Koch, Appl. Phys. Lett. **96**, 221106 (2010).
[5] J. Iveland, L. Martinelli, J. Peretti, J. S. Speck, and C. Weisbuch, Phys. Rev. Lett. **110**, 177406 (2013).
[6] M. Binder, A. Nirschl, R. Zeisel, T. Hager, H.-J. Lugauer, M. Sabathil, D. Bougeard, J. Wagner, and B. Galler, Appl. Phys. Lett. **103**, 071108 (2013).
[7] M. Brendel, A. Kruse, H. Jonen, L. Hoffmann, H. Bremers, U. Rossow, and A. Hangleiter, Appl. Phys. Lett. **99**, 031106 (2011).
[8] B. Galler, P. Drechsel, R. Monnard, P. Rode, P. Stauss, S. Froehlich, W. Bergbauer, M. Binder, M. Sabathil, B. Hahn, and J. Wagner, Appl. Phys. Lett. **101**, 131111 (2012).
[9] D. Schiavon, M. Binder, M. Peter, B. Galler, P. Drechsel, and F. Scholz, Phys. Status Solidi B **250**, 283–290 (2013).
[10] M. Calciatti, M. Goano, F. Bertazzi, M. Vallone, X. Zhou, G. Ghione, M. Meneghini, G. Meneghesso, E. Zanoni, E. Bellotti, G. Verzellesi, D. Zhu, and C. Humphreys, AIP Adv. **4**, 067118 (2014).
[11] G. Kim, J. H. Kim, E. H. Park, D. Kang, and B. G. Park, Opt. Express **22**, 1235–1242 (2014).
[12] R. P. Green, J. J. D. McKendry, D. Massoubre, E. Gu, M. D. Dawson, and A. E. Kelly, Appl. Phys. Lett. **102**, 091103 (2013).
[13] L. Schade, U. T. Schwarz, T. Wernicke, J. Rass, S. Ploch, M. Weyers, and M. Kneiss, Proc. SPIE **8262**, 82620K (2012).
[14] M. Zhang, P. Bhattacharya, J. Singh, and J. Hinckley, Appl. Phys. Lett. **95**, 201108 (2009).
[15] W. Scheibenzuber, U. T. Schwarz, L. Sulmoni, J. Dorsaz, J.-F. Carlin, and N. Grandjean, J. Appl. Phys. **109**, 093106 (2011).
[16] A. David, M. Grundmann, J. F. Kaeding, N. F. Gardner, T. G. Mihopoulos, and M. R. Krames, Appl. Phys. Lett. **92**, 053502 (2008).
[17] H. Y. Ryu, H. S. Kim, and J. I. Shim, Appl. Phys. Lett. **95**, 081114 (2009).
[18] S. Karpov, Opt. Quantum Electron. (published online).
[19] Q. Dai, Q. Shan, J. Wang, S. Chhajed, J. Cho, E. F. Schubert, M. H. Crawford, D. D. Koleske, M. H. Kim, and Y. Park, Appl. Phys. Lett. **97**, 133507 (2010).
[20] A. David and M. J. Grundmann, Appl. Phys. Lett. **96**, 103504 (2010).
[21] J. Hader, J. V. Moloney, and S. W. Koch, Appl. Phys. Lett. **87**, 201112 (2005).
[22] J. Piprek, *Semiconductor Optoelectronic Devices* (Academic Press, San Diego, 2003).
[23] M. Kisin, C. L. Chuang, and H. S. El-Ghoroury, Semicond. Sci. Technol. **27**, 024012 (2012).
[24] B. Galler, H. J. Lugauer, M. Binder, R. Hollweck, Y. Folwill, A. Nirschl, A. Gomez-Iglesias, B. Hahn, J. Wagner, and M. Sabathil, Appl. Phys. Express **6**, 112101 (2013).
[25] APSYS by Crosslight Software, Inc., Vancouver, Canada.
[26] J. Piprek and Z. M. Li, "GaN-based light-emitting diodes," in *Optoelectronic Devices—Advanced Simulation and Analysis*, edited by J. Piprek (Springer, New York, 2005).
[27] J. Pal, G. Tse, V. Haxha, M. A. Migliorato, and S. Tomic, Phys. Rev. B **84**, 085211 (2011).
[28] Quatra/Cels by University of Kassel, Germany.
[29] F. Römer and B. Witzigmann, Opt. Express **22**, A1440 (2014).
[30] E. Kioupakis, Q. Yan, and C. G. Van de Walle, Appl. Phys. Lett. **101**, 231107 (2012).
[31] M. Deppner, F. Römer, and B. Witzigmann, Phys. Status Solidi (RRL) **6**, 418 (2012).
[32] J. Piprek and Z. M. Li, Appl. Phys. Lett. **102**, 131103 (2013).
[33] J. Hader, J. V. Moloney, and S. W. Koch, Appl. Phys. Lett. **92**, 261103 (2008).
[34] E. Kioupakis, P. Rinke, K. T. Delaney, and C. G. Van de Walle, Appl. Phys. Lett. **98**, 161107 (2011).
[35] F. Bertazzi, M. Goano, and E. Bellotti, Appl. Phys. Lett. **101**, 011111 (2012).
[36] F. Bertazzi, X. Zhou, M. Goano, G. Ghione, and E. Bellotti, Appl. Phys. Lett. **103**, 081106 (2013).
[37] F. Bertazzi, X. Zhou, M. Goano, G. Ghione, and E. Bellotti, in *14*th *International Conference on Numerical Simulation of Optoelectronic Devices (NUSOD)* (IEEE, 2014).
[38] R. Vaxenburg, E. Lifshitz, and A. L. Efros, Appl. Phys. Lett. **102**, 031120 (2013).
[39] T. J. Yang, R. Shivaraman, J. S. Speck, and Y. R. Wu, J. Appl. Phys. **116**, 113104 (2014).
[40] A. Hangleiter, T. Langer, M. Gerhard, D. Kalincev, A. Kruse, H. Bremers, U. Rossow, and M. Koch, "Efficiency droop in nitride LED's revisited: Impact of excitonic recombination processes," Proc. SPIE **9363** (to be published).